Assessing spatial variability of thermal conductivity and volumetric heat capacity in hemp-fibred cob walls through in-situ measurements;

Ali Ahmad Waziri[1], Junior Tchiotsop[2], Romain Clerc[1], Nabil Issaadi[1], Philippe Poullain[1], Stéphanie Bonnet[1]

1- *Nantes Université, École Centrale Nantes, CNRS, GeM, UMR 6183, F- 44600 Saint-Nazaire, France.*
2- *Department of Civil Engineering, National Advanced School of Public Works, PO BOX 510, Yaoundé, Cameroon.*

ABSTRACT: Earth-based construction materials are gaining renewed attention for their low environmental impact and favorable thermal behavior, but their intrinsic heterogeneity introduces uncertainty in design and energy modeling. This study investigates the statistical and spatial variability of thermal conductivity (λ) and volumetric heat capacity ($\varrho \cdot Cp$) in a hemp-fibred cob wall through in-situ measurements and geostatistical analysis. A full-scale wall (2.70 m × 1.20 m × 0.10 m) was built using sandy-loam soil from Guérande, France, reinforced with 3% hemp shives by dry mass, and thermal properties were measured at 134 co-located points with the Hot Disk Transient Plane Source technique. Results showed λ values between 0.405–1.010 W/m.K (CV = 17.8%) with a nearly symmetric distribution, while $\varrho \cdot Cp$ ranged from 0.020–1.830 MJ/m³·K (CV = 45.1%) with right-skewness and higher variability. A moderate but significant correlation ($r = 0.36$, $p < 0.001$) was observed between λ and $\varrho \cdot Cp$, reflecting shared dependence on density and porosity but with limited predictive strength. Isotropic empirical variograms shows that both λ and $\varrho \cdot Cp$ vary strongly at short distances, with correlation ranges of about 0.15 m and 0.20 m, respectively. Bootstrap analysis confirmed that the estimates are reliable for λ, while some greater uncertainty remains for $\varrho \cdot Cp$. Overall, the findings highlight strong local variability and short-range correlation in cob materials, supporting the use of fine sampling grids (≈10–15 cm) and the explicit consideration of variability in predictive modeling of earth-based construction.

Keywords: **Cob construction, thermal properties, spatial variability, sustainable building materials.**

1. INTRODUCTION

Growing environmental concerns and stricter energy efficiency requirements are driving the construction industry toward sustainable building materials (Giada et al., 2019; Walker, 2005). Among them, earth-based materials such as cob stand out for their low environmental footprint, local availability, and excellent thermal and moisture buffering capacities (Ciancio and Beckett, 2013). Cob, a mixture of clay-rich soil, sand, water, and fibrous organic matter, has been used in vernacular architecture for centuries and is now experiencing renewed interest in contemporary sustainable construction (Haddad et al., 2024).

Despite these advantages, cob presents unique challenges for engineers and designers. Its intrinsic heterogeneity from natural variations in soil composition, fiber distribution, and construction techniques introduces uncertainty in predicting thermal performance (Zeghari et al., 2021). Conventional approaches often assume homogeneous or isotropic properties, which can lead to inaccurate performance predictions and suboptimal design choices (Ilomets et al., 2017).

Understanding of the spatial variability of thermal properties is therefore essential. It supports more accurate thermal modeling and energy simulation (Yamamoto and Takada, 2022), helps optimize sampling strategies for material characterization, and provides a scientific basis for quality control during construction (Tian et al., 2018).

This study addresses these challenges by conducting comprehensive in-situ measurements of thermal properties in a full-scale hemp-fibred cob wall. The objective is to characterize the spatial variability of two key parameters thermal conductivity (λ) and volumetric heat capacity ($\rho \cdot Cp$) at the wall scale. The analysis covers marginal distributions, statistical correlation, and spatial correlation structures, developed through detailed statistical (Section 3) and geostatistical (Section 4) analyses.

2. Materials and Methods

2.1 Raw Materials

The soil used in this study originated from excavation waste at the Maison Neuve ecological district in Guérande, France, demonstrating the reuse potential of local resources. Standard characterization (NF EN ISO 17892-4) identified a sandy-loam composition with 8% clay, 47% silt, and 45% sand (Figure 2.1a). The complementary GEPPA soil classification (Figure 2.1b) confirmed similar proportions (44% silt and 48% sand), with minor differences attributed to methodological variations.

Atterberg limits testing gave a plastic limit of 17% and a liquid limit of 34%, classifying the soil as moderately plastic and well suited for cob construction, as it balances workability with dimensional stability. The Methylene Blue value (1.9) indicated low clay activity and minimal swelling potential, important for durability under moisture fluctuations.

Hemp shiv was supplied by CHANVRIBAT, with a bulk density of 100–110 kg/m³ and water absorption of 300–450% (Tchiotsop et al., 2022). Fibers had an average length of ~40 mm and were incorporated at 3% of the dry soil mass, following earlier studies that demonstrated optimal trade-offs between thermal performance and structural stability (Glé et al., 2021).

2.2 Wall Construction and Instrumentation

A full-scale cob wall (2.70 m × 1.20 m × 0.10 m) was built in a controlled bi-climatic environment (Figure 2.2a). Construction followed traditional cob techniques, with layers of 50 cm compacted every two days to allow proper curing and minimize cracking (Bui et al., 2014). Dimensional accuracy was ensured using a wood sliding-shuttering system.

The wall was instrumented with SHT75 Sensirion sensors, installed at three depths (25, 50, and 75 mm) and at 21 locations across the surface. Sensors were factory-calibrated and validated against Rotronic references, providing accuracies of ±0.1 °C for temperature and ±2% for relative humidity.

Core samples (Figure 2.2b–c) were extracted using 100 mm dry coring tools, positioned close to the sensor locations to minimize spatial mismatch between in-situ monitoring and laboratory thermal property measurements.

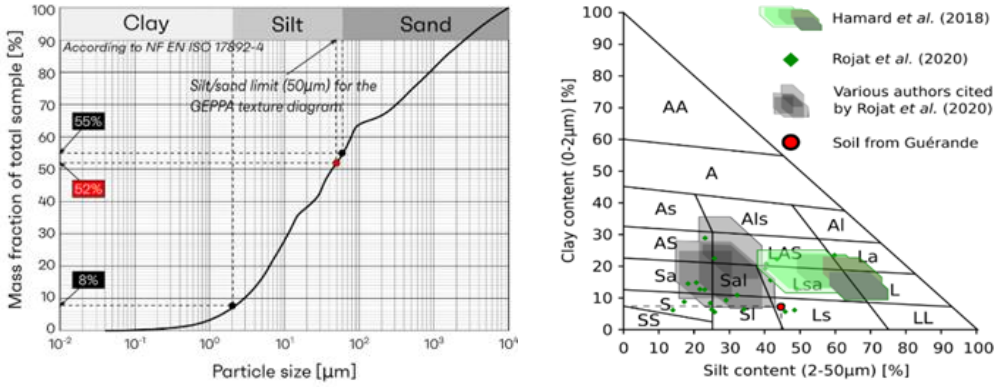

Figure 2.1. Particle size distribution of the soil (a) and "GEPPA" classification of the soil (b)

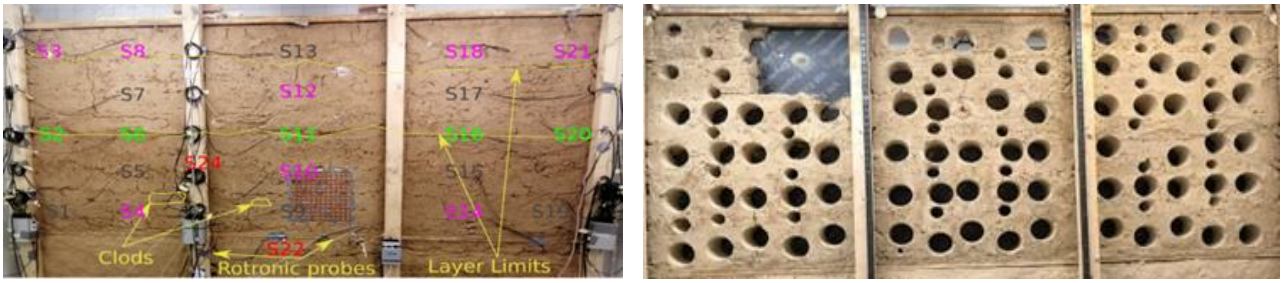

Figure 2.2. Cob Wall (Tchiotsop et al., 2022) (a), Core sampling (b) and spatial location of the specimens (c)

2.3 Thermal Property Measurements Methods

Thermal conductivity (λ) and volumetric heat capacity ($\varrho \cdot Cp$) were measured using the Hot Disk Transient Plane Source (TPS) method (Hot Disk AB, 2015), which determines thermal properties by monitoring temperature evolution at the interface between a heated sensor and the specimen surface (Gustavsson et al., 1994). The TPS system consists of a nickel alloy sensor (10 μm thick) insulated by a Kapton film (30 μm), connected to a power supply, data acquisition unit, and post-processing software.

Before testing, all samples were conditioned at 23 °C and 50% RH until hygrothermal equilibrium was reached, ensuring stable moisture content a critical factor influencing λ and $\varrho \cdot Cp$. Measurements were then performed under controlled laboratory conditions. To avoid air gaps from surface irregularities, the sensor was pressed against specimens using a polyurethane pad in a rubber box, providing uniform contact pressure as shown in Figure 2.3.

Each test applied a constant heating power of 20 mW for 20 s, with temperature rise tracked via resistance changes in the sensor. Thermal properties were inferred from the resulting thermogram using the analytical framework of Gustavsson et al. (1994).

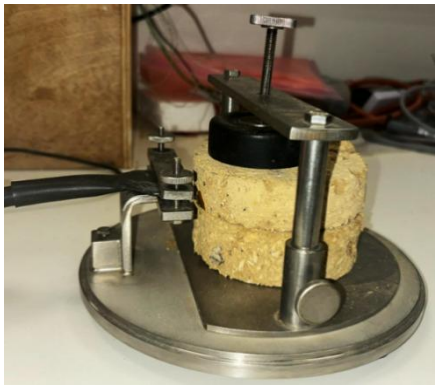

Figure 2.3. Thermal property measurements.

2.4 Geostatistical Methods

Geostatistical methods were applied to characterize and quantify the spatial variability of thermal properties in the hemp-fibred cob wall. Two complementary tools were used: the empirical semi-variogram, which estimates spatial dependence and variability (Diggle and Ribeiro, 2007), and the VARBOOT method, which assesses the uncertainty in this estimate (Pardo-Igúzquiza and Olea, 2012).

Considering isotropy of spatial variability, the empirical semi-variogram $\hat{\gamma}$ is described by Equ. (1). It measures how dissimilarity between paired values changes with lag distance h, with $N(h)$ the number of pairs at lag h, and $Z(x_i)$ and $Z(x_i + h)$ the values at paired locations.

$$\hat{\gamma}(h) = \frac{1}{2N(h)} \sum_{i=1}^{N(h)} [Z(x_i) - Z(x_i + h)]^2 \quad (1)$$

Figure 2.4 shows the key features typically observed in empirical semi-variograms: the **nugget** (microscale variation or measurement uncertainty), the **sill** (total variance, visible only in cases of data stationarity), and the **practical range** (spatial extent of correlation, typically until the limit of 5% correlation between paired values).

To evaluate the robustness of this estimate, the VARBOOT method was employed. Unlike classical bootstrap resampling, VARBOOT preserves spatial dependence by (i) transforming the data into normal scores, (ii) fitting a theoretical covariance model (similar to a theoretical semi-variogram model in cases of data stationarity), and (iii) generating spatially consistent resamples via covariance matrix decomposition. From thousands of resampled datasets, it provides bootstrap medians[1], and confidence intervals of associated empirical semi-variograms, enabling a rigorous uncertainty assessment.

Together, the empirical semi-variogram and the VARBOOT method provide a reliable basis for identifying spatial correlation structures and quantifying uncertainty in the thermal properties of earthen materials.

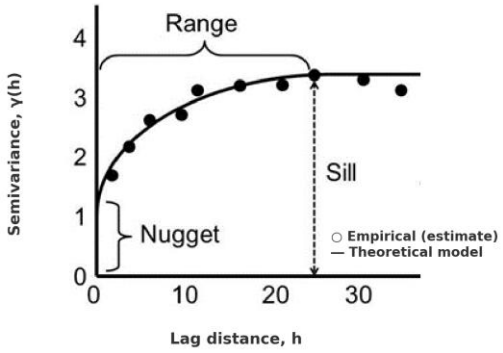

Figure 2.4. Key features typically observed in empirical semi-variograms.

3. Statistical Analysis and Results

3.1 Analysis of marginal distributions

The boxplot of the λ dataset (Figure 3.1b) shows values ranging from 0.405 to 1.010 W/m.K, with a mean of 0.707 W/m.K. The interquartile range (IQR) extends from 0.630 to 0.790 W/m.K. A coefficient of variation (CV) of 17.8% indicates moderate variability. Two low-end outliers, representing about 1.5% of the dataset, suggest localized zones of weaker conduction, possibly linked to porosity or compaction differences. The histogram

[1] identified by authors as a better approximate than bootstrap mean

(Figure 3.1a) confirms a nearly symmetric unimodal distribution, with the majority of values (≈58%) concentrated in the interval [0.63–0.79 W/m.K].

The ϱ·Cp dataset (Figure 3.1d) spans from 0.020 to 1.830 MJ/m³·K, with a mean of 0.783 MJ/m³·K. The IQR extends from 0.528 to 1.065 MJ/m³·K, and the CV reaches 45.1%, indicating strong variability. No outliers are detected, but the histogram (Figure 3.1c) shows that the majority of values (≈62%) fall within [0.50–1.05 MJ/m³·K], with a slightly right-skewed, and apparently bi-modal, distribution.

Overall, λ exhibits relatively controlled variability with near-symmetric distribution, while ϱ·Cp demonstrates higher variability and slight right-skewness. As volumetric heat capacity is derived from λ and thermal diffusivity, measurement uncertainties must be considered. According to ISO 22007-2, Hot Disk (TPS) uncertainty is ~5–7% for λ and ~9–13% for ϱ·Cp (Gustafsson, et al., 2024). For λ, this represents only ~7–15% of the observed CV (17.8%), confirming that most variability reflects material heterogeneity. For ϱ·Cp, the measurement uncertainty explains just ~4–8% of the CV (45.1%), again showing that dispersion is dominated by intrinsic variability rather than instrument error.

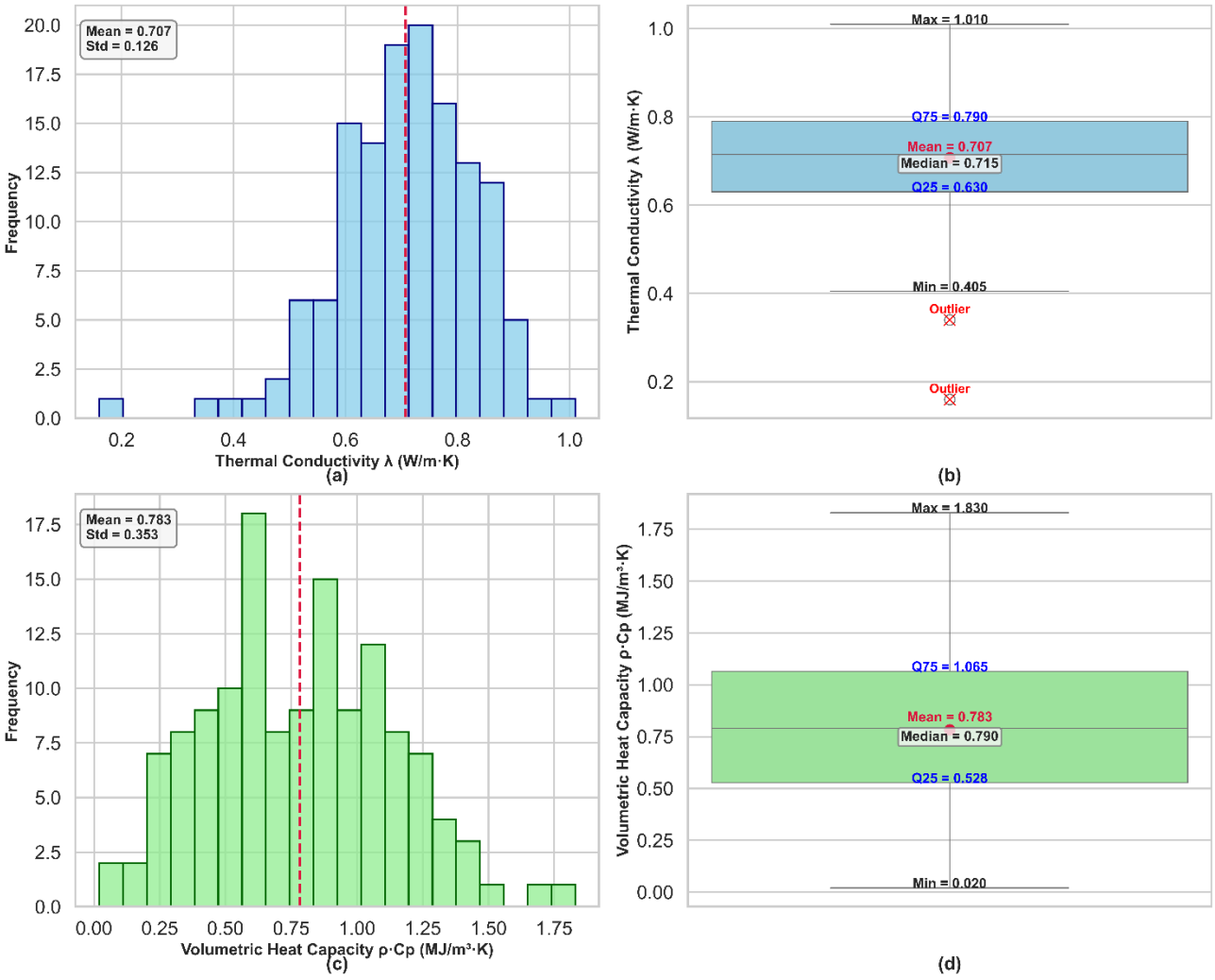

Figure 3.1. Distribution and variability of thermal conductivity (λ) and volumetric heat capacity (ϱ·Cp): (a) Histogram of λ, (b) Boxplot of λ, (c) Histogram of ϱ·Cp, (d) Boxplot of ϱ·Cp.

3.2 Correlation Analysis

The relationship between thermal conductivity (λ) and volumetric specific heat capacity (ϱ·Cp) was investigated using 134 co-located measurements. All available data points were included in the analysis, with outliers retained to reflect the variabilities of both the raw earth material and its building process. The Pearson correlation coefficient of 0.361 indicates a moderate positive linear relationship between λ and ϱ·Cp. This trend is supported by the Spearman rank correlation coefficient of 0.308, which confirms a monotonic association. Both correlations are statistically significant ($p < 0.001$), allowing rejection of the null hypothesis of no correlation.

Despite the statistical significance, the strength of the correlation remains limited. The coefficient of determination ($R^2 \approx 0.13$) suggests that only about 13% of the variance in ϱ·Cp can be explained by λ, leaving the majority of variability unaccounted for. This highlights that while a relationship exists, λ is not a reliable predictor of ϱ·Cp on its own. Physically, the observed moderate correlation aligns with the fact that both λ and ϱ·Cp are influenced by common microstructural factors such as density, porosity, and compaction. However, the relatively low explanatory power reflects the complexity of heat storage and transfer mechanisms in heterogeneous earthen materials.

In summary, the analysis demonstrates that λ and ϱ·Cp share a statistically significant but modest correlation, both statistically and physically meaningful, yet insufficient to establish a strong predictive link between the two properties.

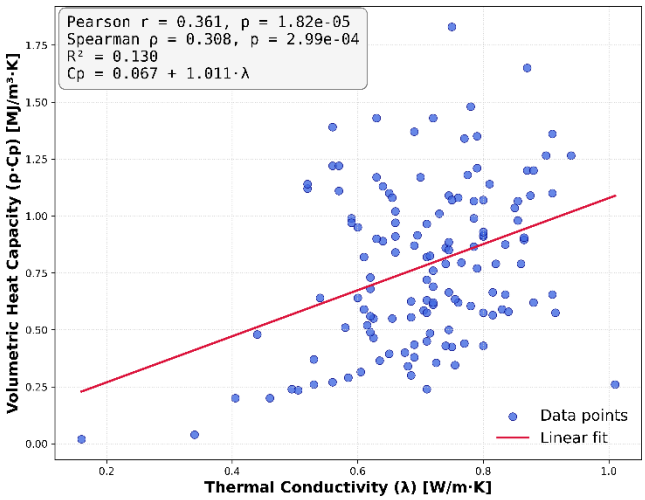

Figure 3.2. Correlation analysis of thermal conductivity and volumetric heat capacity

4. Geostatistical Analysis

4.1 Spatial Distribution of Thermal Properties

The spatial distribution of the measured thermal properties across the cob wall is presented in Figures 3.3a and 3.3b. The measurement grid covers wall lengths from 0 to 2.7 m and heights from 0 to 1.2 m, with individual points corresponding to the exact coring locations used for laboratory characterization.

For thermal conductivity (λ), values range approximately between 0.2 and 1.0 W/m·K, while volumetric heat capacity (ϱ·Cp) spans from about 0.2 to 1.8 MJ/m³·K. Both datasets display a scattered distribution across the wall surface, without any consistent horizontal or vertical gradient. Instead, the variation is localized, with higher and lower values appearing in close proximity, reflecting the inherent heterogeneity of the cob mixture.

The lack of large-scale directional trends supports the assumption of second-order stationarity, which will be verified through empirical semi-variogram estimations. Moreover, the use of groups of observation points with small spacing provides a solid basis for subsequent geostatistical analysis and modeling of thermal properties (Bachoc, 2014).

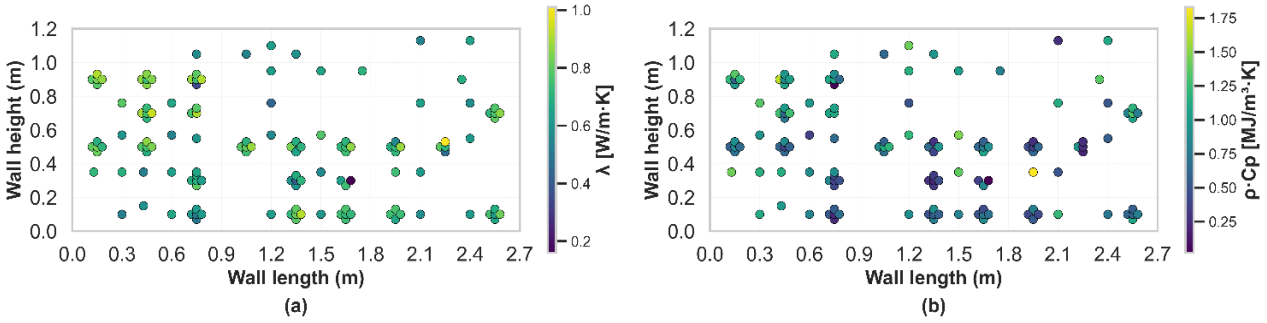

Figure 4.1. Spatial distribution of the thermal properties in the wall: (a) thermal conductivity (b) volumetric heat capacity

4.2 Empirical Semi-Variogram Analysis and Uncertainty Assessment

Figures 4.1a–b shows the isotropic empirical semi-variograms of thermal conductivity (noted $\hat{\gamma}_{\lambda}(h)$) and volumetric heat capacity (noted $\hat{\gamma}_{\rho C_p}(h)$). Each estimation is annotated with the associated number of data pairs $N(h)$. Both $\hat{\gamma}_{\lambda}(h)$ and $\hat{\gamma}_{\rho C_p}(h)$ exhibit short practical ranges and sills that match total sample variances of the variables (≈0.016 (W/m.K)² for λ and ≈0.124 (MJ/m³·K)² for ϱ·Cp). This last point tends to confirm the assumption of second-order stationarity.

According to Figure 4.1a, $\hat{\gamma}_{\lambda}(h)$ increases sharply from the origin, ranging between 0.011 and 0.020 (W/m.K)². Instead of flattening smoothly, the curve shows oscillations, A local maximum occurs near h≈0.225 m followed by a dip around 0.30–0.40 m before returning to the sill at larger lags. Despite these fluctuations, the overall sill remains consistent with the total variance (~0.016(W/m.K)²). The relatively low values at the first lag (0.075 m, 119 pairs) and the rapid increase to the sill suggests existence of spatial correlation for lags under a short practical range of about 0.18–0.22 m,.

According to Figure 4.1b, $\hat{\gamma}_{\rho C_p}(h)$ shows a pronounced small-lag structure: a low first lag (~0.075 m, N(h)=119) followed by a sharp peak at h≈0.14 m (N(h)=147) reaching ~0.15 (MJ/m³·K)², then a smooth plateau of ~0.11–0.13 (MJ/m³·K)² from 0.25 to 0.60 m. This behavior suggests existence of spatial correlation for lags under a slighlty longer practical range of 0.18–0.24 m.

To confirm existence of spatial correlation for both λ and ϱ·Cp at short lags and determine the meanings of observed oscillations, we perform a bootstrap-based uncertainty assessment of empirical semi-variogram, using the VARBOOT program. Note that (i) among classical covariance models[2], the spherical one is the only one which leads to no rejection of normality hypothesis for standardized data, and (ii) following Pardo-Igúzquiza and Olea advice, bootstrap-median is used as the central estimator. 2000 bootstrap samples were used.

Figures 4.1c–d shows bootstrap-medians of empirical semi-variograms along with their 95% confidence intervals. We first note their consistence: for λ, the bootstrap median closely follows the empirical semi-variogram at short lags but lie slightly above it at distances >0.25 m, which may imply underestimation of the variance at long ranges due to limited $N(h)$ values. For ϱ·Cp, the bootstrap median tracks the empirical semi-variogram well and converges to a sill near 0.145, consistent with the total variance. For both λ and ϱ·Cp, the range of the 95% confidence intervals consistently varies with $N(h)$, being widest at low $N(h)$ values (e.g., at >0.2 m with $N(h)$~119–147), and tightest at high ones (0.25–0.50 m, with $N(h)$~300–500). This explains the oscillations in the empirical semi-variograms, which mainly reflect fluctuations in data density rather than non-stationarity.

[2] namely, exponential, gaussian, and spherical

Indeed, we observe that the bootstrap medians and their 95% confidence intervals exhibit clear stationary random field behavior with sills consistent with their total variances. Additionally, their growth is evident for spacings between 0 and ~0.15–20 cm, confirming the presence of spatial correlation for both λ and $\varrho \cdot Cp$. Thus, measurements separated by more than ~0.15–0.20 m can be considered effectively independent.

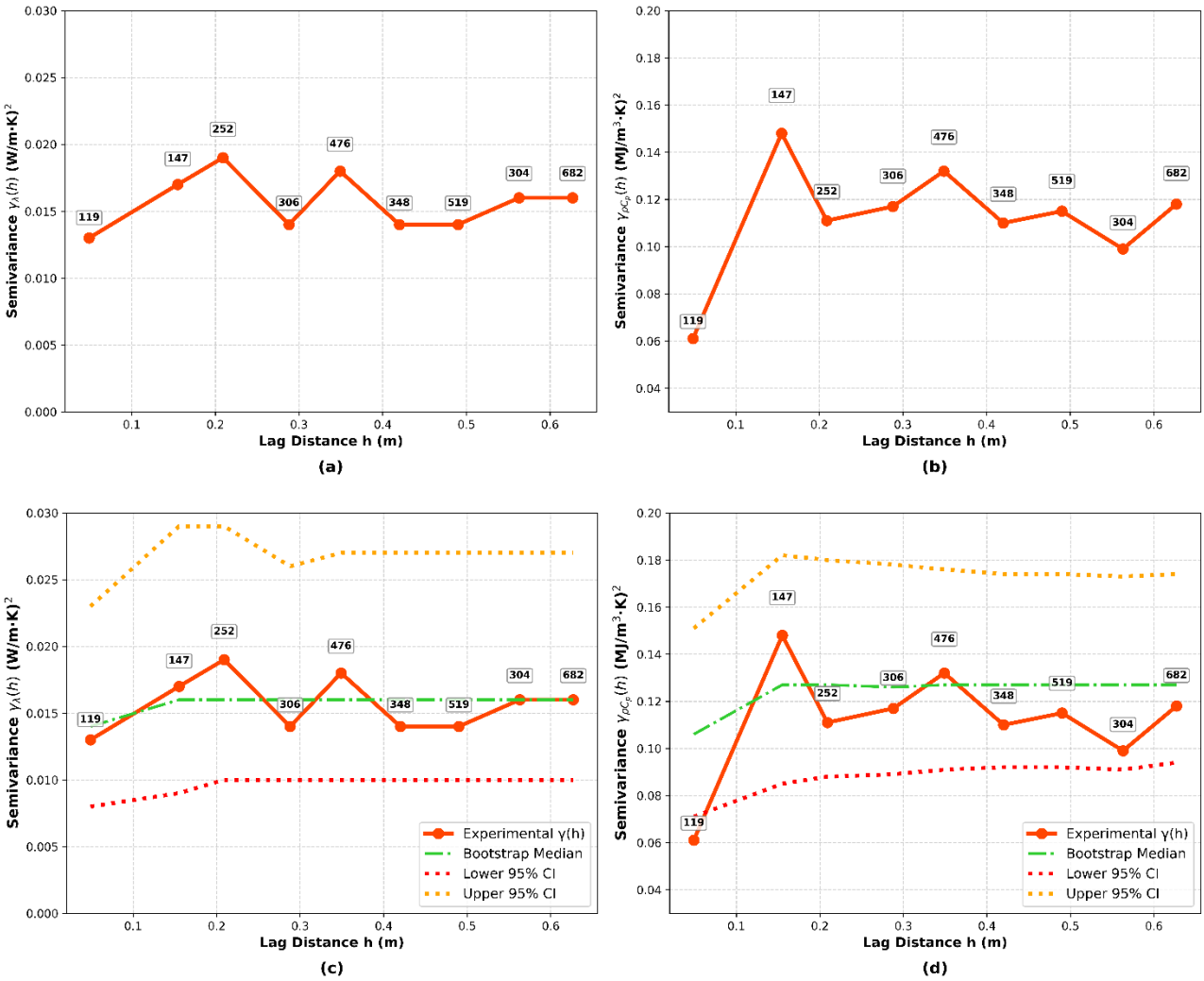

Figure 4.2. Empirical variogram of the thermal conductivity (a) and the volumetric heat capacity (b). Uncertainty assessment of the empirical variogram for thermal conductivity using VARBOOT (c) and for volumetric heat capacity (d). Numbers in boxes above each point indicate the number of data pairs used in the estimation at each lag.

5. Conclusions

This study provides a detailed characterization of the statistical and spatial variability of thermal conductivity (λ) and volumetric heat capacity ($\varrho \cdot Cp$) in hemp-fibred cob, using 134 in-situ measurements supported by geostatistical analysis.

Key findings include:

1. **Statistical variability:**

- λ ranged from 0.405 to 1.010 W/m.K with CV = 17.8%, showing moderate variability and near-symmetric distribution.
- $\varrho \cdot Cp$ ranged from 0.020 to 1.830 MJ/m³·K with CV = 45.1%, exhibiting higher dispersion and slight right-skewness.

2. **Statistical correlation:** λ and $\varrho \cdot Cp$ were moderately correlated ($r = 0.36$, $R^2 \approx 0.13$, $p < 0.001$), consistent with their shared dependence on material density and porosity. However, λ alone cannot reliably predict $\varrho \cdot Cp$.

3. **Spatial variability:**

- Empirical semi-variograms associated to their bootstrap-based uncertainty assessment demonstrated existence of short-range spatial correlation with practical ranges of ~0.15–0.20 m for both λ and $\varrho \cdot Cp$.
- Both semi-variograms stabilized at sills equal to their sample total variances, confirming stationarity of the underlying random fields. This however do not confirm isotropy of spatial variability, which should be further explored.

Implications:

- The analysis shows that the thermal properties of cob exhibit short-range spatial variability, with practical ranges of ~0.15–0.20 m. Consequently, measurements spaced beyond ~0.20 m can be treated as effectively independent.
- For wall-scale investigations, a sampling interval of ~10–15 cm is suggested to adequately capture this variability and enable robust geostatistical modeling of earthen materials (Uzielli et al., 2006).
- It is expected that incorporating this quantified variability into building performance simulations will improve the accuracy of energy modeling and durability predictions for earth-based construction systems.

Overall, this research uses a robust methodological framework for combining field measurements, statistical analysis, and geostatistics to capture the variability of cob materials. The insights gained provide a foundation for more reliable performance-based design of sustainable building envelopes using earth-based construction.

References:

Bachoc, F., 2014. Asymptotic analysis of the role of spatial sampling for covariance parameter estimation of Gaussian processes. J. Multivar. Anal. 125, 1–35. https://doi.org/10.1016/j.jmva.2013.11.015

Bui, Q.B., Morel, J.-C., Hans, S., Walker, P., 2014. Effect of moisture content on the mechanical characteristics of rammed earth. Constr. Build. Mater. 54, 163–169. https://doi.org/10.1016/j.conbuildmat.2013.12.067

Ciancio, D., Beckett, C., 2013. Rammed earth: An overview of a sustainable construction material.

Giada, G., Caponetto, R., Nocera, F., 2019. Hygrothermal Properties of Raw Earth Materials: A Literature Review. Sustainability 11, 5342. https://doi.org/10.3390/su11195342

Glé, P., Lecompte, T., Hellouin De Ménibus, A., Lenormand, H., Arufe, S., Chateau, C., Fierro, V., Celzard, A., 2021. Densities of hemp shiv for building: From multiscale characterisation to application. Ind. Crops Prod. 164, 113390. https://doi.org/10.1016/j.indcrop.2021.113390

Gustavsson, M., Karawacki, E., Gustafsson, S.E., 1994. Thermal conductivity, thermal diffusivity, and specific heat of thin samples from transient measurements with hot disk sensors. Rev. Sci. Instrum. 65, 3856–3859. https://doi.org/10.1063/1.1145178

Haddad, K., Lannon, S., Latif, E., 2024. Investigation of Cob construction: Review of mix designs, structural characteristics, and hygrothermal behaviour. J. Build. Eng. 87, 108959. https://doi.org/10.1016/j.jobe.2024.108959

Ilomets, S., Kalamees, T., Vinha, J., 2017. Indoor hygrothermal loads for the deterministic and stochastic design of the building envelope for dwellings in cold climates. J. Build. Phys. 41, 174425911771844. https://doi.org/10.1177/1744259117718442

NF EN ISO 17892-4 [WWW Document], n.d. . Afnor Ed. URL https://www.boutique.afnor.org/en-gb/standard/nf-en-iso-178924/geotechnical-investigation-and-testing-laboratory-testing-of-soil-part-4-de/fa166662/80069 (accessed 9.11.25).

Pardo-Igúzquiza, E., Olea, R.A., 2012. VARBOOT: A spatial bootstrap program for semivariogram uncertainty assessment. Comput. Geosci. 41, 188–198. https://doi.org/10.1016/j.cageo.2011.09.002

Tchiotsop, J., Issaadi, N., Poullain, P., Bonnet, S., Belarbi, R., 2022. Assessment of the natural variability of cob buildings hygric and thermal properties at material scale: Influence of plants add-ons. Constr. Build. Mater. 342, 127922. https://doi.org/10.1016/j.conbuildmat.2022.127922

Tian, W., Heo, Y., Wilde, P., Li, Z., Yan, D., Park, C.-S., Feng, X., Augenbroe, G., 2018. A review of uncertainty analysis in building energy assessment. Renew. Sustain. Energy Rev. 93, 285–301. https://doi.org/10.1016/j.rser.2018.05.029

Uzielli, M., Lacasse, S., Nadim, F., Phoon, K.-K., 2006. Soil Variability Analysis for Geotechnical Practice, Characterisation and Engineering Properties of Natural Soils. https://doi.org/10.1201/NOE0415426916.ch3

Walker, P. (Ed.), 2005. Rammed earth: design and construction guidelines. BRE Bookshop, Watford.

Yamamoto, H., Takada, S., 2022. Influence of variability in hygrothermal properties on analytical results of simultaneous heat and moisture transfer in porous materials. J. Build. Phys. 45, 757–773. https://doi.org/10.1177/17442591211034194

Zeghari, K., Gounni, A., Louahlia, H., Marion, M., BOUTOUIL, M., Goodhew, S., Streiff, F., 2021. Novel Dual Walling Cob Building: Dynamic Thermal Performance. Energies 14, 7663. https://doi.org/10.3390/en14227663